It is not certain, however, which factor is more important in the initiation step, i.e., the rate or efficiency of initiation. A quantitative treatment of this problem should therefore be performed.

Conclusions

The 2,4,5-trisubstituted isomers of 1,3-dioxolan-2-ylium salts presented above were found to be new and interesting initiators for the polymerization of trioxane. They were shown to initiate the polymerization via simple monomer cationation, a considerable effect of the structure of the cation being found.

References and Notes

(1) Jedliński, Z.; Łukaszczyk, J. *Macromolecules* **1975**, *8*, 700.
(2) Jedliński, Z.; Łukaszczyk, J.; Dudek, J.; Gibas, M. *Macromolecules* **1976**, *9*, 622.
(3) Gibas, M.; Jedliński, Z. *Pol. J. Chem.* **1978**, *52*, 435.
(4) Smirnov, Yu. N.; Volkov, V. P.; Oleynik, E. F.; Komarov, B. A.; Rosenberg, B. A.; Enikolopyan, N. S. *Vysokomol. Soedin., Ser. A* **1974**, *16*, 735.
(5) Penczek, S. *Makromol. Chem.* **1974**, *175*, 1217.
(6) Pittman, C. U., Jr; McManus, S. P.; Larsen, J. W. *Chem. Rev.* **1972**, *72*, 357.
(7) Jedliński, Z.; Łukaszczyk, J., in preparation.
(8) Hart, H.; Tomalia, D. A. *Tetrahedron Lett.* **1966**, 3383.

Effect of Stiffness on the First Cumulant and Polymer Dimensions in Solution

M. Benmouna and A. Ziya Akcasu*

Department of Nuclear Engineering, The University of Michigan,
Ann Arbor, Michigan 48109

M. Daoud

CEA, Centre d'Etudes Nucléaires de Saclay, Gif-sur-Yvette, France.

Received June 16, 1980

ABSTRACT: The first cumulant of the intermediate scattering function, the hydrodynamic radius, and the radius of gyration are calculated in the case of linear stiff chains. Two different models are used to characterize chain stiffness: broken-chain and sliding-rod models. The crossover from flexible to rodlike behavior in the intermediate-q region is investigated. It is found that, in the Rouse limit, $\Omega \sim q^{2+1/\nu}$ for $qbn < 1$ and q^3 for $qbn > 1$, where $\nu = {}^1/_2$ or ${}^3/_5$, depending on whether the solvent conditions correspond to Θ or good solvent. In the Zimm limit, $\Omega \sim q^3$ for $qbn < 1$ but $\Omega \sim q^3 \ln (1/qb)$ for $qbn > 1$. Hence, the intermediate asymptotic region is now divided into two subasymptotic regions due to the presence of a rodlike behavior for $qbn > 1$. The diffusion coefficient in the small-q region is also investigated. These results are useful in the interpretation of light and neutron scattering experiments.

I. Introduction

In this paper we investigate the effect of chain stiffness on various properties of polymer solutions. Specifically, we calculate the static structure factor, the radius of gyration, the first cumulant, and the hydrodynamic radius for stiff chains. The chain stiffness is included through the equilibrium distribution function in monomer configuration space because dynamic properties such as the first cumulant are expressed, in the present formalism, in terms of static correlation functions. The calculations are carried out for two chain models: The first is the broken-chain model in which the actual polymer is represented by a sequence of rods connected together by universal joints. Each rod contains an equal number of monomers distributed along the rod at equal distances. This model may be realistic for molecules such as DNA. The second is the sliding-rod model, in which the polymer is treated around each monomer locally as a rod of chemical length n but as a flexible Gaussian chain for chemical lengths larger than n. The length of the rod at each monomer represents the local stiffness of the actual chain. As opposed to the broken-chain model, the locations of the rods relative to the chain are not fixed in this model but rather allowed to slide along the chain from monomer to monomer. The sliding-rod model, which is inspired by the "blob" concept introduced recently in chain statistics,[1,2] may be interpreted as a discrete version of the conventional wormlike-chain representation[3] of polymer molecules. It may be a realistic description of polyelectrolytes in solutions.[4]

The main motivation of this paper is to calculate the first cumulant, including stiffness, for all values of q, with particular attention to the transition from a single rod to a completely flexible-chain behavior. Our purpose is not to reexamine, with a slightly modified model, the equilibrium properties of stiff chains which have already been studied extensively in the literature[3-8] but rather to study the effect of stiffness on some dynamical properties (e.g., first cumulant in the intermediate-q range) which have been accessible experimentally only recently by dynamic light[9] and neutron[10] scattering techniques. In this sense, the present work is an extension of our previous work based on linear response theory to stiff chains. The first cumulant of the intermediate scattering function is given by[11]

$$\Omega(q) = \langle \rho^* \mathcal{L} \rho \rangle / \langle \rho^* \rho \rangle \tag{1}$$

where ρ is the monomer density in Fourier space. $\mathcal{L}$ is the dynamical operator that governs the time dependence of ρ, and $\langle\ \rangle$ denotes thermal average with respect to the equilibrium distribution in polymer configuration space.

This expression of Ω can accommodate any choice of the equilibrium distribution and the dynamical operator $\mathcal{L}$. We have used it extensively to investigate the effect of temperature and concentration on the dynamical properties of linear flexible polymers in solution, in the framework of Kirkwood–Riseman theory.[9,11-14] Others[15] have extended these calculations to branched polymers. In the present calculation we use the same dynamical model[16,17] with two different equilibrium distributions appropriate for the broken-chain and sliding-rod chain models that take into account the chain stiffness. The bond-length and bond-angle constraints involved in these

0024-9297/80/2213-1703$01.00/0

chain models are included in the calculation of Ω only at the end through the equilibrium distribution when performing equilibrium averages, but not in the dynamical operator. This procedure corresponds to modeling the constraints as the limit of "soft" potentials determining bond length and bond angle, to singular potentials at the end. As pointed out by Stockmayer and Burchard[18] recently, it might be more accurate, especially in the single-rod limit, to introduce the constraints at the outset by modifying the dynamical operator $\mathcal{L}$, following Fixman and Kovac's[19] prescription, which has been scrutinized very recently by Helfand.[20] We have not adopted this procedure because the chain is treated as flexible as a whole in the sliding-rod model except for small local sections that are approximated as rods, and the calculation of Ω becomes intractable when the dynamical operator $\mathcal{L}$ with constraints is used in (1). This problem has also been discussed briefly by Akcasu and co-workers in ref 9. When the Kirkwood-Riseman Fokker-Planck operator is adopted, eq (1) becomes[11]

$$\Omega(q) = \frac{\sum_{jl} \langle \mathbf{D}(\mathbf{R}_{jl}) e^{i\mathbf{q}\cdot\mathbf{R}_{jl}} \rangle : \mathbf{qq}}{\sum_{jl} \langle e^{i\mathbf{q}\cdot\mathbf{R}_{jl}} \rangle} \tag{2}$$

where $\mathbf{D}(\mathbf{R}_{jl})$ is the diffusion tensor. This form shows more clearly that one needs only the equilibrium distribution of the vector distance $\mathbf{R}_{jl}$ between two monomers to calculate Ω.

II. Broken-Chain Model

A. Calculation of the Static Form Factor. We consider a broken chain formed of N rods connected together by universal joints. Each rod contains n monomers distributed at equal distances along its axis. The total number of monomers in the chain is $\mathcal{N} \equiv Nn + 1$. The density of monomers can be written as

$$\rho = \sum_{j=1}^{N} \sum_{\alpha=0}^{n-1} e^{i\mathbf{q}\cdot(\mathbf{R}_j + \alpha \mathbf{b}_j)} + e^{i\mathbf{q}\cdot\mathbf{R}_{N+1}} \tag{3}$$

The static form factor $\langle \rho^* \rho \rangle$ appearing in the denominator of Ω (cf. eq 2) is obtained as

$$\langle \rho^*\rho \rangle = 1 + 2\sum_{j=1}^{N}\sum_{\alpha=0}^{n-1} \langle e^{i\mathbf{q}\cdot(\mathbf{R}_{N+1} - \mathbf{R}_j - \alpha\mathbf{b}_j)} \rangle + \sum_{j\alpha}\sum_{l\beta} \langle e^{i\mathbf{q}\cdot(\mathbf{R}_j - \mathbf{R}_l + \alpha\mathbf{b}_j - \beta\mathbf{b}_l)} \rangle \tag{4}$$

A detailed calculation of these sums is reproduced in Appendix I. The final result is

$$\langle \rho^*\rho \rangle = 1 + NS_n^{\mathrm{rod}}(qb) + 2Nj_0^{-1}(qbn)S[S + 1 - j_0(qbn)]G_N[j_0(qbn)] - 2S[S - j_0(qbn)][1 - j_0^{N}(qbn)][1 - j_0(qbn)]^{-1} \tag{5a}$$

where

$$j_0(x) \equiv \sin x / x \tag{5b}$$

$$S \equiv \sum_{\alpha=1}^{n} j_0(qb\alpha) \tag{5c}$$

$$G_N(x) \equiv \frac{x}{1-x}\left[1 - \frac{x}{N}\frac{(1-x^N)}{(1-x)}\right] \tag{5d}$$

$$S_n^{\mathrm{rod}}(x) \equiv n + 2\sum_{\alpha=1}^{n}(n-\alpha)j_0(x\alpha)$$

or

$$S_n^{\mathrm{rod}}(x) = n - nj_0(xn) + 2nS - n(xn/2)j_0^2(xn/2)\ \mathrm{ct}\ (x/2) \tag{5e}$$

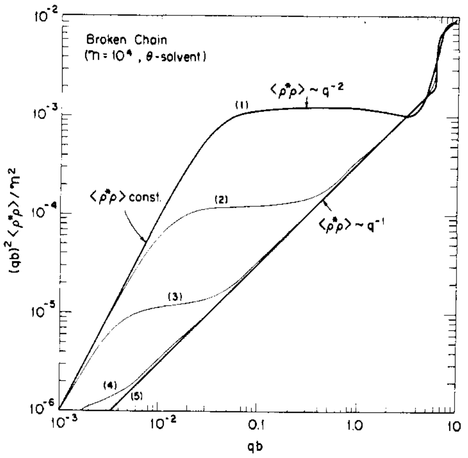

Figure 1. Variation of $(qb)^2\langle \rho^*\rho \rangle / \mathcal{N}^2$ with qb for a broken chain under Θ conditions ($\mathcal{N} = 10^4$): curve 1, $\mathcal{N}/n = 10^4$, freely jointed; curve 2, $\mathcal{N}/n = 10^3$; curve 3, $\mathcal{N}/n = 10^2$; curve 4, $\mathcal{N}/n = 1$, single rod; curve 5, the asymptotic behavior, $(\pi/\mathcal{N})qb$. This fiqure shows the crossover from flexible ($\langle \rho^*\rho \rangle \sim q^{-2}$) to rodlike ($\langle \rho^*\rho \rangle \sim q^{-1}$) behavior in the intermediate q region. The curves are very similar to those obtained by Koyama[7] using the wormlike-chain model.

Special Cases. 1. Freely Jointed Chain (n = 1). By letting $n = 1$ in eq 5 we recapture the static form factor for a freely jointed chain of N segments, i.e.

$$\langle \rho^*\rho \rangle_{\mathrm{fj}} = N\left[\frac{N+1}{N} + 2G_N(j_0(qb))\right] \tag{6}$$

which was obtained and studied by Akcasu and Higgins[21] previously.

2. Single Rod (N = 1). By replacing N by 1 in eq 5, we obtain the static form factor for a single rod of $n + 1$ monomers

$$\langle \rho^*\rho \rangle_{\mathrm{sr}} = S_{n+1}^{\mathrm{rod}}(qb) \tag{7}$$

which can be expressed as

$$\langle \rho^*\rho \rangle_{\mathrm{sr}} = n + 1 - nj_0(qbn) + 2(n+1)S - n(qbn/2)j_0^2(qbn/2)\ \mathrm{ct}\ (qb/2) \tag{8a}$$

Letting $b \to 0$, $n \to \infty$ but keeping nb finite and replacing the sums by integrals, this expression of $\langle \rho^*\rho \rangle$ reduces to the well-known form[22,31]

$$\frac{\langle \rho^*\rho \rangle}{n^2} = \frac{2}{qL}\int_0^{qL} \mathrm{d}x\ \frac{\sin x}{x} - \left[\frac{2}{qL}\sin{(qL/2)}\right]^2 \tag{8b}$$

where

$$L \equiv nb$$

The asymptotic behavior in the intermediate-q region is obtained from this expression with $qL \to 0$ as

$$n^{-2}\langle \rho^*\rho \rangle = \pi/qL \tag{8c}$$

We will come back to the single-rod calculations in a later section.

In Figure 1 we plot $(qb)^2\langle \rho^*\rho \rangle/\mathcal{N}^2$ as a function of qb (Kratky plot) for various rod lengths to investigate the effect of stiffness on the static form factor. The points to be made in this figure are as follows: In the intermediate-q range ($qR_{\mathrm{G}} \gg 1$ and $qb \ll 1$) $\langle \rho^*\rho \rangle$ behaves like q^{-2} for $qbn < 1$, which is characteristic of a flexible unperturbed chain. For $qbn > 1$, however, $\langle \rho^*\rho \rangle \sim q^{-1}$. This behavior is due to the rodlike structure of the chain, probed in this q region. The curves show that the q^{-1} region extends more as the rod length nb becomes larger. For both small ($qR_{\mathrm{G}} < 1$) and large q values ($qb > 1$) $\langle \rho^*\rho \rangle$ is a constant equal to $\mathcal{N}^2$ and $\mathcal{N}$, respectively. Note the oscillatory tendency of $\langle \rho^*\rho \rangle$ with a period 2π, which is characteristic behavior for freely jointed chains. These oscillations are due to

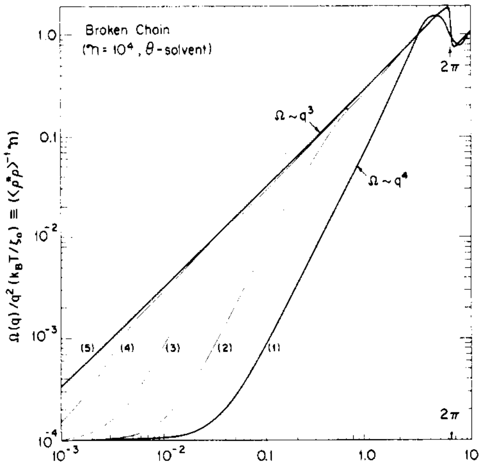

Figure 2. Variation of $\Omega(q)/q^2(k_BT/\xi_0)$ with qb for a broken chain under Θ conditions and in the Rouse limit ($\mathcal{N} = 10^4$): curve 1, $\mathcal{N}/n = 10^4$, freely jointed; curve 2, $\mathcal{N}/n = 10^3$; curve 3, $\mathcal{N}/n = 10^2$; curve 4, $\mathcal{N}/n = 1$, single rod; curve 5, the asymptotic behavior, qb/π. This figure also shows the crossover from the flexible ($\Omega \sim q^4$) to rodlike ($\Omega \sim q^3$) behavior in the intermediate q region.

$j_0(qbn)$ in the expression of $\langle \rho^* \rho \rangle$.

B. First Cumulant Ω(*q*). 1. Rouse Limit. In the absence of hydrodynamic interaction (Rouse limit), the normalized first cumulant $\Omega(q)/q^2(k_BT/\xi_0)$ is merely the inverse of the static form factor times the total number of monomers $\mathcal{N}$, i.e.

$$\frac{\Omega(q)}{q^2(k_BT/\xi_0)} = \mathcal{N}(\langle \rho^* \rho \rangle)^{-1} \tag{9}$$

In Figure 2 we have plotted $\Omega(q)/q^2(k_BT/\xi_0)$ as a function of qb for the same values of n and $\mathcal{N}$ as in Figure 1. There are three regions of q where Ω has a characteristic behavior. (i) $qR_G < 1$. This is the region of q where the probing radiation "sees" the diffusion of the whole chain and $\Omega(q) = q^2(k_BT/\mathcal{N}\xi_0)$. (ii) The intermediate-$q$ region ($qR_G \gg 1$ and $qb \ll 1$) where Ω shows a crossover from the flexible unperturbed chain result $\Omega \sim q^4$ for $qbn \ll 1$ to the rodlike result $\Omega \sim q^3$ for $qbn \gg 1$, the latter becoming dominant when n is of the order of $\mathcal{N}$. We observe an interesting analogy between the effects of excluded volume and stiffness:[4,23] Recall that the excluded-volume exponent ν, according to Flory's formula, is $^3/_5$ when the dimensionality of space is 3, and $\nu = 1$ when the dimensionality is 1. In the case of a Gaussian chain in a good solvent, $\Omega \sim q^{2+1/\nu}$ in the Rouse limit.[2,12] The flexible-chain result, $\Omega \sim q^{11/3}$, is obtained with $\nu = {}^3/_5$, whereas the rodlike behavior, $\Omega \sim q^3$, follows with $\nu = 1$. This result is a direct consequence of the behavior of $\langle \rho^* \rho \rangle$ in the intermediate-q region, i.e., $\langle \rho^* \rho \rangle \sim q^{-1/\nu}$, which gives q^{-1} when $\nu = 1$. (iii) In the high-q region ($qb > 1$), $\Omega(q) \approx q^2k_BT/\xi_0$ with a sudden change at $qb = 2\pi$, as explained above.

2. Zimm Limit. The first cumulant Ω in the presence of hydrodynamic interaction can also be expressed in terms of the static form factor, $S(q) \equiv N^{-1}\langle \rho^* \rho \rangle$, by rewriting eq 2 as follows:[24]

$$\Omega(q) = \frac{k_BT}{\xi_0}\mathbf{qq}{:}\left[\frac{\mathbf{I}}{S(q)} + \frac{\xi_0}{(2\pi)^3}\int \mathrm{d}^3\, k\, \mathbf{T}(\mathbf{q}-\mathbf{k})\frac{S(k)-1}{S(q)}\right] \tag{10a}$$

where $\mathbf{T}(\mathbf{q})$ is the Fourier transform of the Oseen tensor; i.e.

$$\mathbf{T}(\mathbf{q}) = \frac{1}{\eta_0 q^2}\left[\mathbf{I} - \frac{\mathbf{qq}}{q^2}\right] \tag{10b}$$

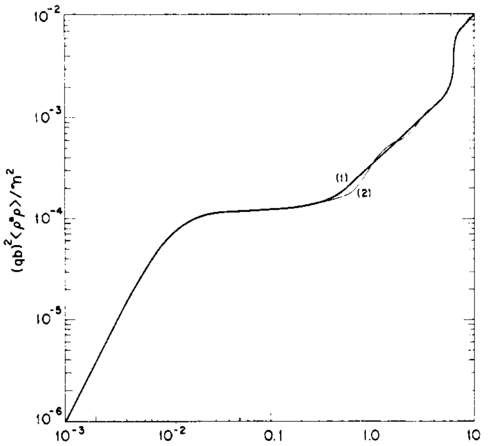

Figure 3. Variation of $(qb)^2\langle \rho^* \rho \rangle/\mathcal{N}^2$ with qb under Θ conditions ($\mathcal{N} = 10^4$, $\mathcal{N}/n = 10^3$): curve 1, broken-chain model; curve 2, sliding-rod model. This figure shows that the static form factors are almost identical in both models.

This expression clearly shows that the calculation of Ω is reduced, in the framework of the Kirkwood–Riseman theory of solution dynamics, to the calcualtion of the static form factor $S(q)$, which is an equilibrium property of the medium, even though Ω is a dynamical quantity. The implications of this form from a theoretical point of view are important, in particular, in conjunction with the scaling properties of dynamical quantities. It shows how the equilibrium and dynamic scaling laws may be related to each other.

The first cumulant was previously calculated for $n = 1$ (freely jointed chain) in the presence of hydrodynamic interaction, using eq 10.[21] However, the extension of such a calculation to cases where $n > 1$ (broken chain) involves intractable manipulations. One may consult for this matter the calculation of the diffusion coefficient for broken and wormlike chains by Hearst and Stockmayer.[17] Here, we use the sliding-rod model to include the effect of the hydrodynamic interaction in the calculation of Ω. The results obtained with the broken-chain and sliding-rod models cannot differ from each other significantly because they yield practically identical values for the static form factor, as demonstrated in Figure 3.

III. Sliding-Rod Model

The sliding-rod concept is introduced into the mathematical formulation as an equilibrium distribution model for the vector distance $\mathbf{R}_{jl} \equiv \mathbf{R}_j - \mathbf{R}_l$, as follows:

$$\langle e^{i\mathbf{q}\cdot\mathbf{R}_{jl}} \rangle = \frac{\sin\,[qb(j-l)]}{qb(j-l)} \qquad \text{if } |j-l| \le n \tag{11a}$$

and

$$\langle e^{i\mathbf{q}\cdot\mathbf{R}_{jl}} \rangle = \exp(-q^2\langle |\mathbf{R}_{jl}|^2 \rangle/6) \qquad \text{if } |j-l| \ge n \tag{11b}$$

where

$$\langle |\mathbf{R}_{jl}|^2 \rangle = \left(\frac{|j-l|}{n}\right)^{2\nu} n^2b^2 \tag{11c}$$

and $\nu = {}^3/_5$ in the good-solvent limit and $^1/_2$ in the Θ-solvent limit. For intermediate temperatures or concentrations, we can follow exactly the same procedure as in ref 12 and 13.

A. Calculation of the First Cumulant. By substituting (11) into (2) and performing some simple algebraic transformations,[12] we obtain the normalized first cumulant as

$$\frac{\Omega(q)}{q^2(k_\mathrm{B}T/\xi_0)} = \left[1 + \left(\frac{\xi_0}{\eta_0 b}\right)\left(\frac{qb}{2\pi}\right)\sum_{m=1}^{n-1}\left(1 - \frac{m}{\mathcal{N}}\right)f_1(qbm) + \left(\frac{\xi_0}{\eta_0 b}\right)\left(\frac{qb}{4\pi^{3/2}}\right)\sum_{m=n}^{\mathcal{N}-1}\left(1 - \frac{m}{\mathcal{N}}\right)f_2(x_m)\right] \Big/ \left[1 + 2\sum_{m=1}^{n-1}\left(1 - \frac{m}{\mathcal{N}}\right)\frac{\sin(qbm)}{qbm} + 2\sum_{m=n}^{\mathcal{N}-1}\left(1 - \frac{m}{\mathcal{N}}\right)\exp(-x_m{}^2)\right] \tag{12a}$$

where

$$f_1(x) \equiv \frac{1}{4x}\int_{-1}^{1}\mathrm{d}\mu\,(1 + \mu^2)e^{ix\mu} \tag{12b}$$

which is also equal to

$$f_1(x) \equiv \frac{1}{x^2}\left[\sin x - \frac{(\sin x - x\cos x)}{x^2}\right] \tag{12c}$$

and

$$f_2(x) \equiv \frac{1}{x^2}\left[-\frac{1}{x} + \left(2 + \frac{1}{x^2}\right)e^{-x^2}\int_0^x \mathrm{d}u\,e^{u^2}\right] \tag{12d}$$

$$x_m{}^2 \equiv \left(\frac{m}{n}\right)^{2\nu} q^2b^2n^2/6 \tag{12e}$$

If we let $n = 1$ in (12) we recapture the results for a flexible Gaussian chain reported in ref 11 and 14. The single-rod limit is obtained by letting $n = \mathcal{N}$. In the numerical computations we have used this form of the first cumulant which involves exact summations. In order to study various limiting cases, analytically, we approximate the sums by integrals. A word of caution is that the numerical accuracy of replacing sums by integrals may not be sufficient for q values outside the asymptotic region. However, the accuracy may be improved somewhat by using the trapezoidal rule or other integration schemes. Since we use the analytical results only to discuss asymptotic limits, we do not include these refinements in the following integral form of $\Omega(q)$, which is obtained from (12):

$$\frac{\Omega(q)}{q^2(k_\mathrm{B}T/\xi_0)} = \left[1 + \left(\frac{\xi_0}{\eta_0 b}\right)\left(\frac{1}{2\pi}\right)\int_{Q_1}^{Q_n}\mathrm{d}x\left(1 - \frac{x}{Q_\mathcal{N}}\right)f_1(x) + \left(\frac{\xi_0}{\eta_0 b}\right)\left(\frac{1}{4\nu\pi^{3/2}}\right)\frac{Q_\mathcal{N}}{\kappa^{1/\nu}}\int_{Q_n}^{\kappa}\mathrm{d}x\left(1 - \frac{x^{1/\nu}}{\kappa^{1/\nu}}\right)x^{(1-\nu)/\nu}f_2\left(\frac{x}{\sqrt{6}}\right)\right] \Big/ \left[1 + \frac{2}{Q_1}\int_{Q_1}^{Q_n}\mathrm{d}x\left(1 - \frac{x}{Q_\mathcal{N}}\right)\frac{\sin x}{x} + \frac{2}{\nu}\frac{Q_\mathcal{N}}{Q_1\kappa^{1/\nu}}\int_{Q_n}^{\kappa}\mathrm{d}x\left(1 - \frac{x^{1/\nu}}{\kappa^{1/\nu}}\right)x^{(1-\nu)/\nu}e^{-x^2/6}\right] \tag{13a}$$

where

$$Q_p \equiv qbp \tag{13b}$$

and

$$\kappa \equiv (\mathcal{N}/n)^\nu Q_n \tag{13c}$$

$f_1(x)$ and $f_2(x)$ are given by (12c) and (12d), respectively. If we let $n = 1$ in eq 13a, the first integral in both the numerator and the denominator vanishes, so that we recapture the Ω for a flexible Gaussian chain which was derived previously by Akcasu and co-workers.[11,14] We do not discuss this limit here any further. In the single-rod limit we let $n = \mathcal{N}$ in (13) and obtain

$$\frac{\Omega(q)}{q^2(k_\mathrm{B}T/\xi_0)} = \left[1 + \left(\frac{\xi_0}{\eta_0 b}\right)\left(\frac{1}{2\pi}\right) \times \int_{Q_1}^{Q_\mathcal{N}}\mathrm{d}x\left(1 - \frac{x}{Q_\mathcal{N}}\right)\frac{1}{x^2}\left(\sin x - \frac{(\sin x - x\cos x)}{x^2}\right)\right] \Big/ \left[1 + \frac{2}{Q_1}\int_{Q_1}^{Q_\mathcal{N}}\mathrm{d}x\left(1 - \frac{x}{Q_\mathcal{N}}\right)\frac{\sin x}{x}\right] \tag{14}$$

The exponent ν does not appear in this form of Ω since excluded-volume effects are irrelevant in the case of rodlike molecules. In the absence of hydrodynamic interaction (Rouse limit), we let $(\xi_0/\eta_0 b) = 0$ in (14) and obtain

$$\frac{\Omega(q)}{q^2(k_\mathrm{B}T/\xi_0)} = \left[1 + \frac{2}{Q_1}\int_{Q_1}^{Q_\mathcal{N}}\mathrm{d}x\left(1 - \frac{x}{Q_\mathcal{N}}\right)\frac{\sin x}{x}\right]^{-1} \tag{15}$$

The single-rod problem was investigated by many workers. For example, Pecora[22] has obtained the static form factor as well as $S(q,t)$ for a single rod in both the discrete- and continuous-chain cases. However, he has not computed the initial slope $\Omega(q)$ of the normalized $S(q,t)$ explicitly.

In the small-q limit, where both Q_1 and $Q_\mathcal{N}$ are smaller than 1, we recapture the standard diffusion result

$$\Omega(q) = D(\mathcal{N})q^2 \tag{16a}$$

where

$$D(\mathcal{N}) = k_\mathrm{B}T/\mathcal{N}\xi_0 \tag{16b}$$

In the intermediate-q range ($Q_1 \to 0$ and $Q_\mathcal{N} \to \infty$) we have

$$\Omega(q) = \frac{1}{\pi}\left(\frac{k_\mathrm{B}T}{\xi_0/b}\right)q^3 \tag{17}$$

This result is valid when $b \to 0$, $\mathcal{N} \to \infty$, keeping the total length of the rod constant. Since $\xi_0\mathcal{N}$ is the total friction coefficient, ξ_0/b can be interpreted as the friction coefficient per unit length of the rod and, hence, must be treated as finite in the continuous limit. The q^3 dependence of Ω is due to the q^{-1} behavior of the static form factor in the intermediate region. Recall once more that for flexible chains, we obtain $\Omega \sim q^{2+1/\nu}$, which yields $\Omega \sim q^4$ in a Θ solvent and $q^{11/3}$ in a good solvent. The $\Omega \sim q^3$ dependence indicates a certain analogy between stiffness effect and excluded-volume effect, if one uses an adjusted exponent $\nu = 1$, as we have pointed out in an earlier section. In the limit where hydrodynamic interaction becomes predominant (Zimm limit), eq 14 reduces to

$$\frac{\Omega(q)}{(qb)^2(k_\mathrm{B}T/\eta_0 b^3)} = \frac{1}{2\pi}\left\{\int_{Q_1}^{Q_\mathcal{N}}\mathrm{d}x\left(1 - \frac{x}{Q_\mathcal{N}}\right)\frac{1}{x^2}\left[\sin x - \frac{(\sin x - x\cos x)}{x^2}\right] \Big/ \left[1 + \frac{2}{Q_1}\int_{Q_1}^{Q_\mathcal{N}}\mathrm{d}x\left(1 - \frac{x}{Q_\mathcal{N}}\right)\frac{\sin x}{x}\right]\right\} \tag{18}$$

since for small-q values ($Q_1 \to 0$ and $Q_{\mathcal{N}} \to 0$)

$$\lim_{x\to 0} \frac{1}{x^2}\left[\sin x - \frac{(\sin x - x\cos x)}{x^2} \right] = \frac{2}{3x} \tag{19}$$

We obtain the usual diffusional relaxation frequency $\Omega(q) = D(\mathcal{N})q^2$, where $D(\mathcal{N})$ is the translational diffusion coefficient. For large $\mathcal{N}$ it reduces to the form

$$D(\mathcal{N}) = \frac{1}{3\pi}\frac{k_BT}{\eta_0 b}\frac{\ln \mathcal{N}}{\mathcal{N}} \tag{20}$$

which is a known result,[3,17] for the translational diffusion of rodlike molecules, within the framework of Kirkwood–Riseman theory. It contains contributions of both the parallel and perpendicular diffusion of the rod; i.e., $D = (D_{\parallel} + 2D_{\perp})/3$. The $(\ln \mathcal{N})/\mathcal{N}$ term is a characteristic feature of the diffusion of elongated rigid bodies such as elongated ellipsoids[25,26] and long cylinders.[27] It should be pointed out that Ω given in eq 13 contains the contributions of both translational diffusion and internal modes, i.e., rotational diffusion in the case of rods, for larger values of q.

In the intermediate-q region, we have

$$\Omega(q) = \frac{1}{2\pi^2}\frac{k_BT}{\eta_0}q^3 \times \lim_{Q_1\to 0}\int_{Q_1}^{\infty}\frac{\mathrm{d}x}{x^2}\left[\sin x - \frac{(\sin x - x\cos x)}{x^2} \right] \tag{21}$$

In Appendix II, we show the details of this integration. The result is

$$\Omega(q) = \frac{1}{3\pi^2}\frac{k_BT}{\eta_0}q^3 \ln (1/qb) \tag{22}$$

As in the case of translational diffusion, here also we find a logarithmic factor. If we use the trapezoidal rule in replacing the sums by integrals and keep the constants, we obtain

$$\Omega(q) = \frac{1}{3\pi^2}\frac{k_BT}{\eta_0}q^3[\ln (1/qb) + 0.756] \tag{23}$$

which is numerically more accurate when qb is not in the asymptotic region. In the case of a chain formed of a large number of rods of a certain length nb such that $1 < n \ll \mathcal{N}$, and in the region of q accessible in light scattering experiments, i.e., $qbn \to 0$ but $\kappa \equiv (\mathcal{N}/n)^{\nu}qbn$ finite, eq 13 can be written as

$$\frac{\Omega(q)}{q^2D(\nu)} = \frac{3(1-\nu)(2-\nu)}{16\nu}{\kappa_\nu}^{(\nu-1)/\nu}\int_0^{{\kappa_\nu}^2}\mathrm{d}u\left(1 - \frac{u^{1/2\nu}}{{\kappa_\nu}^{1/\nu}}\right)\frac{1}{u^{2-1/2\nu}} \times \left[-\frac{1}{\sqrt{u}} + \left(2 + \frac{1}{u}\right)e^{-u}\int_0^{u^{1/2}}\mathrm{d}t\ e^{t^2} \right] \times \left(\int_0^1 \mathrm{d}u\ (1-u)e^{-u^{2\nu}{\kappa_\nu}^2}\right)^{-1} \tag{24a}$$

where

$$D(\nu) = \frac{k_BT}{\eta_0 R_G(\nu)}\{\pi(1-\nu)(2-\nu)[3\pi(1+\nu)(1+2\nu)]^{1/2}\}^{-1} \tag{24b}$$

$${\kappa_\nu}^2 = \tfrac{1}{3}(1+\nu)(1+2\nu)q^2{R_G}^2(\nu) \tag{24c}$$

and

$$R_G(\nu) = bn\left(\frac{\mathcal{N}}{n}\right)^{\nu}\frac{1}{[2(1+\nu)(1+2\nu)]^{1/2}} \tag{24d}$$

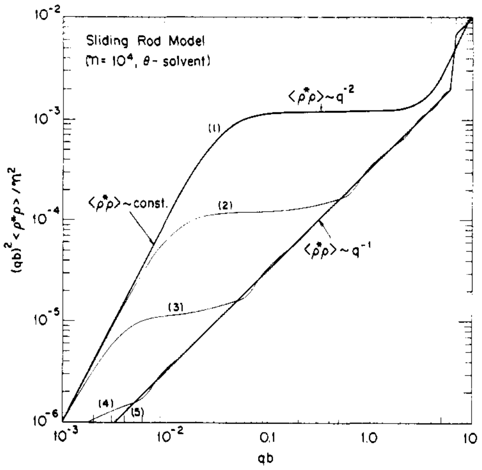

Figure 4. Variation of $(qb)^2\langle\rho^*\rho\rangle/\mathcal{N}^2$ with qb in the sliding-rod model under Θ conditions ($\mathcal{N} = 10^4$): curve 1, $\mathcal{N}/n = 10^4$, Gaussian chain; curve 2, $\mathcal{N}/n = 10^3$; curve 3, $\mathcal{N}/n = 10^2$; curve 4, $\mathcal{N}/n = 1$, single rod; curve 5, the asymptotic behavior, $(\pi/\mathcal{N})qb$. This figure is almost identical with Figure 1.

These results were obtained by Akcasu et al.[11,14] in the limit of $n = 1$. In fact (24) is identical with their result if the number of statistical units N is identified as $(\mathcal{N}/n)$. In particular, in the intermediate-q region where $\kappa_\nu \to \infty$, we recapture

$$\Omega(q) = 0.0625\frac{k_BT}{\eta_0}q^3 \quad \text{for } \nu = \tfrac{1}{2}\ (\Theta \text{ solvent}) \tag{25a}$$

and

$$\Omega(q) = 0.0789\frac{k_BT}{\eta_0}q^3 \quad \text{for } \nu = \tfrac{3}{5}\ (\text{good solvent}) \tag{25b}$$

which were reported earlier.[14]

Finally, for high-q values, we always obtain the segmental diffusion frequency with a certain oscillatory pattern due to the sudden change in $\langle\rho^*\rho\rangle$ at $qb = 2\pi$, as explained previously.

In Figure 4 we have plotted $(qb)^2\langle\rho^*\rho\rangle/\mathcal{N}^2$ vs. qb for five values of n varying from $n = 1$ (flexible Gaussain chain) to $n = \mathcal{N}$ (single rod), in Θ-solvent conditions. These curves are practically identical with the broken-chain case illustrated in Figure 3.

Figure 5 shows the normalized first cumulant as a function of qb for various values of n and in the presence of hydrodynamic interaction ($\xi_0/\eta_0 b = 3\pi$). The $n = 1$ curve (Gaussian flexible) has already been reported and discussed elsewhere.[11,14] The $n = 10$ ($\mathcal{N}/n = 10^3$) curve behaves like a Gaussian flexible chain for all q's such that $qbn < 1$, i.e., when $qbn(\mathcal{N}/n)^{1/2} < 1$, $\Omega(q) = D(n,\mathcal{N})q^2$, where $D(n,\mathcal{N}) = 0.195(k_BT/\eta_0 bn)[1/(\mathcal{N}/n)^{1/2}]$, and when $qbn(\mathcal{N}/n)^{1/2} > 1$ but $qbn < 1$ we have $\Omega \sim 0.0625q^2$, whereas when $qbn > 1$ we have $\Omega \sim (1/3\pi^2)q^3 \ln (1/qb)$, as shown by eq 22. For the cases $\mathcal{N}/n = 100$ and 1, represented by curves 3 and 4, the behavior of Ω with q is even more affected by the dominant rodlike structure of the chain. To illustrate the effects of excluded-volume interaction, we have plotted in Figure 6 $\Omega(q)/(qb)^2(k_BT/\eta_0 b^3)$ vs. qb for $\xi_0/\eta_0 b = 3\pi$ and $n = 100$ ($\mathcal{N}/n = 100$). As we would expect, Ω is practically insensitive to temperature for $qbn > 1$ since in the rigid part of the chain, excluded-volume effects are irrelevant. In the q region defined

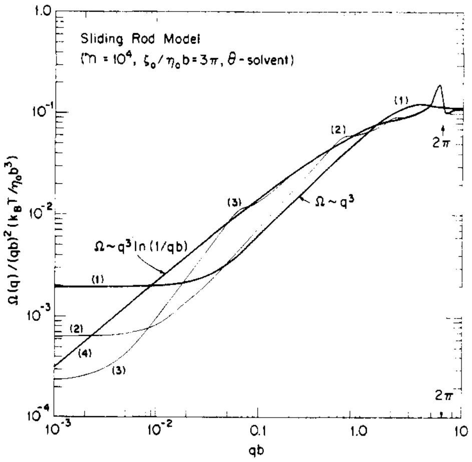

Figure 5. Variation of $\Omega(q)/(qb)^2(k_BT/\eta_0b^3)$ with qb in the sliding-rod model under Θ conditions with nonpreaveraged Oseen tensor ($\mathcal{N} = 10^4$, $\xi_0/\eta_0b = 3\pi$): curve, 1, $\mathcal{N}/n = 10^4$, Gaussian chain; curve 2, $\mathcal{N}/n = 10^3$; curve 3, $\mathcal{N}/n = 10^2$; curve 4, $\mathcal{N}/n = 1$, single rod. This curve shows the crossover from flexible ($\Omega \sim q^3$) to rodlike [$\Omega \sim q^3 \ln (1/qb)$] behavior in the intermediate q region when hydrodynamic interaction is predominant. We have not shown the case $\mathcal{N}/n = 10$ for clarity.

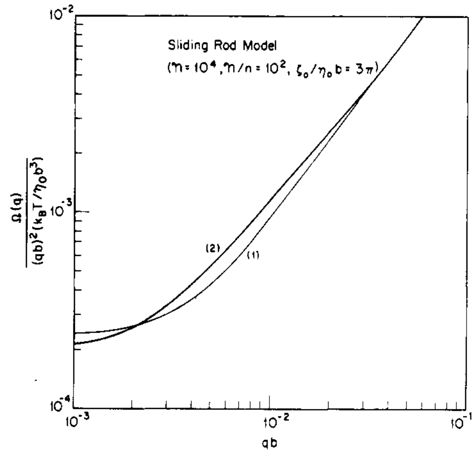

Figure 6. Variation of $\Omega(q)/(qb)^2(k_BT/\eta_0b^3)$ with qb in the sliding-rod model with nonpreaveraged Oseen tensor ($\mathcal{N} = 10^4$, $\mathcal{N}/n = 10^2$, $\xi_0/\eta_0b = 3\pi$): curve 1, Θ solvent ($\nu = {}^1/_2$); curve 2, good solvent ($\nu = {}^3/_5$). This figure shows that practically only the flexible part of the chain ($qbn < 1$) is affected by temperature.

by $qbn < 1$, the shape of Ω follows the standard form, namely

$$\Omega(q) = 0.0789 \frac{k_BT}{\eta_0} q^3 \quad \text{for } qbn(\mathcal{N}/n)^{1/2} > 1 \tag{26a}$$

and

$$\Omega(q) = D(n,\mathcal{N})q^2 \quad \text{for } qbn(\mathcal{N}/n)^{1/2} < 1 \tag{26b}$$

where $D(n,\mathcal{N})$ is given above.

B. Calculation of the Molecular Dimensions. 1. Radius of Gyration. In this calculation we follow the procedure of ref 28, with a slight generalization in the definition of the quantity $\langle|\mathbf{R}_m|^2\rangle$, which we write as follows:

$$\langle|\mathbf{R}_m|^2\rangle = m^{2\nu'}b^2 \quad \text{if } m \leq n \tag{27a}$$

and

$$\langle|\mathbf{R}_m|^2\rangle = (m/n)^{2\nu}B^2 \quad \text{if } m \geq n \tag{27b}$$

with

$$B^2 = n^{2\nu'}b^2 \tag{27c}$$

This form of $\langle|\mathbf{R}_m|^2\rangle$ represents a crossover from a regime of chain statistics characterized by an exponent ν' below a chemical length cutoff n to another regime characterized by ν above n. Such a model, known as the blob model, which was introduced first by one of us,[1] has already been applied in the literature[1,2,12-14,28] to investigate the temperature and concentration effects on various dynamic and static properties of polymer solutions. In the temperature blob model $\nu' = {}^1/_2$ and $\nu = {}^3/_5$, whereas in the concentration case $\nu' = {}^3/_5$ and $\nu = {}^1/_2$. In this paper, we are concerned with the stiffness effects which may arise from the chemical structure of the chain, and for other reasons such as electrostatic interactions (e.g., polyelectrolytes). Thus, for our problem $\nu' = 1$ and $\nu = {}^3/_5$ or ${}^1/_2$, depending on whether the solvent conditions correspond to good or Θ solvent.

Substituting (27) into the definition of R_G

$$R_G^2 = \frac{1}{\mathcal{N}^2} \sum_{m=1}^{\mathcal{N}} (\mathcal{N} - m)\langle|\mathbf{R}_m|^2\rangle \tag{28}$$

We can easily verify that

$$\frac{R_G^2}{\mathcal{N}^{2\nu'}b^2} = \left[\frac{x^{2\nu'+1}}{2\nu'+1} - \frac{x^{2(\nu'+1)}}{2(\nu'+1)}\right] + x^{2(\nu'-\nu)}\left[\frac{1 - x^{2\nu+1}}{2\nu+1} - \frac{1 - x^{2(\nu+1)}}{2(\nu+1)}\right] \tag{29}$$

where $x \equiv n/\mathcal{N}$. If we set $\nu' = {}^1/_2$, we recapture the temperature blob result of Akcasu and Han.[28] In the present problem $\nu' = 1$ so that (29) becomes

$$\alpha_s^2(x) = x^3(4 - 3x) + 12x^{2(1-\nu)}\left[\frac{1 - x^{2\nu+1}}{2\nu+1} - \frac{1 - x^{2(\nu+1)}}{2(\nu+1)}\right] \tag{30}$$

where

$$\alpha_s(x) \equiv R_G(x)/R_G(\text{rod } \mathcal{N})$$

and

$$R_G(\text{rod } \mathcal{N}) = \mathcal{N}b/\sqrt{12} \tag{31}$$

If $n = 1$ and $\mathcal{N}$ is much larger than 1, eq (30) yields the known result

$$R_G(\text{flexible}) = \frac{\mathcal{N}^{\nu}b}{[2(1+\nu)(1+2\nu)]^{1/2}} \tag{32}$$

Taking the ratio of (32) and (31) yields

$$\alpha_s(\text{flexible}) = \left[\frac{6}{(1+\nu)(1+2\nu)}\right]^{1/2} \mathcal{N}^{\nu-1} \tag{33a}$$

or

$$\alpha_s(\text{flexible, }\Theta) = 2^{1/2}\mathcal{N}^{-0.5} \quad (\nu = 1/2) \tag{33b}$$

and

$$\alpha_s(\text{flexible, good}) = 1.3\mathcal{N}^{-0.4} \quad (\nu = 3/5) \tag{33c}$$

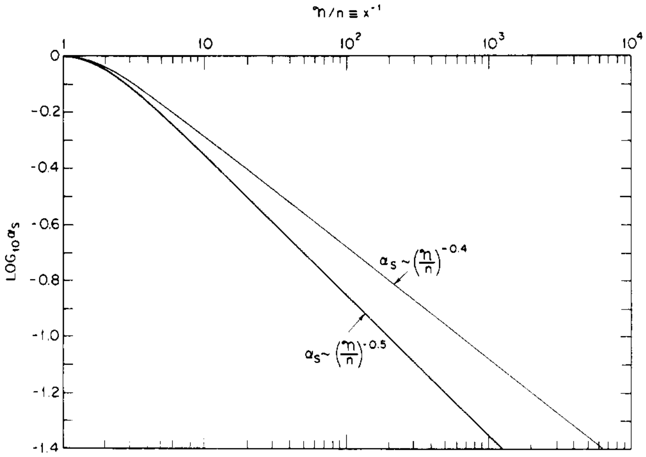

Figure 7. Variation of $\alpha_s(x)$ with $x^{-1} \equiv \mathcal{N}/n$ in the sliding-rod model under Θ (curve 1) and good-solvent (curve 2) conditions.

For large $\mathcal{N}/n$ we obtain the asymptotic form of α_s from eq 30 as

$$\alpha_s \to \left[\frac{6}{(1+\nu)(1+2\nu)}\right]^{1/2}\left(\frac{\mathcal{N}}{n}\right)^{\nu-1} \tag{34a}$$

or

$$\alpha_s \to 2^{1/2}(\mathcal{N}/n)^{-0.5} \qquad (\nu = 1/2) \tag{34b}$$

and

$$\alpha_s \to 1.3(N/n)^{-0.4} \qquad (\nu = 3/5) \tag{34c}$$

Figure 7 shows the variation of α_s as function of $\mathcal{N}/n \equiv x^{-1}$ both in Θ- and good-solvent conditions.

2. Hydrodynamic Radius. The hydrodynamic radius is defined by[28]

$$R_H = k_BT/6\pi\eta_0 D \tag{35}$$

where D is obtained from eq 13 in the limit of small q

$$D = \lim_{q\to 0}\,[\Omega(q)/q^2] \tag{36}$$

(It is pointed out by Fixman[32] that D in (36) is the short-time diffusion coefficient, about 1.6% larger than the long-time translational diffusion coefficient.) The result for large $\mathcal{N}$ is

$$D = \frac{k_BT}{\mathcal{N}\xi_0}\left[1 + \frac{1}{3\pi}\left(\frac{\xi_0}{\eta_0 b}\right)\ln n + \frac{2}{(6\pi)^{1/2}\pi}\left(\frac{\xi_0}{\eta_0 b}\right)\left(\frac{x^{\nu-1}-1}{1-\nu} - \frac{x^{\nu-1}-x}{2-\nu}\right)\right] \tag{37}$$

Introducing the dynamic "coiling" factor $\alpha_H(x) \equiv R_H(x)/R_H(\text{rod } \mathcal{N})$ and keeping the Zimm term only, we can cast these results in the form

$$\alpha_H(x,\mathcal{N}) = \left\{1 + \frac{1}{\ln \mathcal{N}}\left[\ln x + \left(\frac{6}{\pi}\right)^{1/2}\left(\frac{x^{\nu-1}-1}{1-\nu} - \frac{x^{\nu-1}-x}{2-\nu}\right)\right]\right\}^{-1} \tag{38}$$

where the hydrodynamic radius for a rod of length $\mathcal{N}b$ is (see eq 20 and 35)

$$R_H(\text{rod } \mathcal{N}) = \mathcal{N}b/(2 \ln \mathcal{N}) \tag{39}$$

Note that α_H does not depend on x only but depends also on $\mathcal{N}$ explicitly through $\ln \mathcal{N}$. For a flexible coil ($n = 1$, $\mathcal{N}$ large)

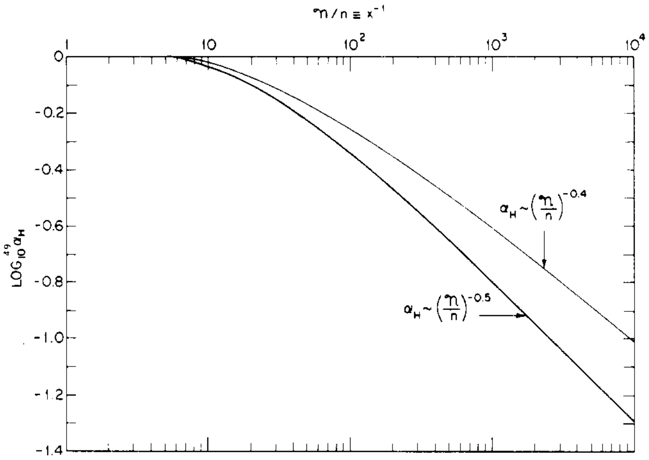

Figure 8. Variation of $\alpha_H(x)$ with $x^{-1} \equiv \mathcal{N}/n$ ($\mathcal{N} = 10^4$) in the sliding-rod model under Θ (curve 1) and good-solvent (curve 2) conditions.

$$R_H(\text{flexible } \mathcal{N}) = \frac{(6\pi)^{1/2}}{12}(1-\nu)(2-\nu)\mathcal{N}^{\nu}b \tag{40}$$

so that the ratio of (40) and (39) yields

$$\alpha_H(\text{flexible}) = \left(\frac{\pi}{6}\right)^{1/2}(1-\nu)(2-\nu)\mathcal{N}^{\nu-1}\ln \mathcal{N} \tag{41}$$

For large $\mathcal{N}/n$, the asymptotic behavior of $\alpha_H(x)$ is

$$\alpha_H \to \left(\frac{\pi}{6}\right)^{1/2}(1-\nu)(2-\nu)\left(\frac{\mathcal{N}}{n}\right)^{\nu-1}\ln \mathcal{N} \tag{42a}$$

or

$$\alpha_H \to 0.543(\mathcal{N}/n)^{-0.5}\ln \mathcal{N} \qquad (\nu = 1/2) \tag{42b}$$

and

$$\alpha_H \to 0.405(\mathcal{N}/n)^{-0.4}\ln \mathcal{N} \qquad (\nu = 3/5) \tag{42c}$$

Figure 8 shows the variation of $\alpha_H(x)$ as a function of x for $\mathcal{N} = 10^4$, both in Θ- and good-solvent conditions. These plots show that the asymptotic dependence of α_H on x^{-1} is practically not affected by $\ln \mathcal{N}$ term for large $\mathcal{N}/n$.

We can readily extend these calculations to intermediate temperature but the results are identical with those of ref 28; therefore, we do not reproduce them here.

In the case of broken chain, we calculated R_G, using (28), as

$$R_G^2 = \frac{n^4N(N+1)(N-1)b^2}{6(Nn+1)^2} + \frac{(n+2)(n+1)^2nNb^2}{12(Nn+1)^2} - \frac{n^2(n^2-3n-1)(N-1)N}{6(Nn+1)^2}b^2 \tag{43}$$

The details are presented in Appendix III. This is an exact expression for the radius of gyration of a broken chain which is valid under Θ conditions and for any values of n and N. In particular, for a freely jointed chain ($n = 1$)

$$R_G^2(\text{fj}) = \frac{N(N+2)}{6(N+1)}b^2 \tag{44a}$$

which yields the following result[3] for large N:

$$R_G^2(\text{fj}) = Nb^2/6 \tag{44b}$$

In the case of a single rod, $N = 1$ so that (43) becomes

$$R_G^2 = n(n+2)(b^2/12) \tag{45a}$$

or, for large n

$$R_G^2 = n^2b^2/12 \qquad (45b)$$

This is also a known result for rigid rods.[8,22,29] For a dumbbell ($N = 1$ and $n = 1$), (41a) yields $R_G = b/2$. We can consider more complicated cases such as once, twice, ... multiple broken chains by assigning different values for N in (45).

IV. Conclusion

The main theme of this work is to study the effect of stiffness on the first cumulant $\Omega(q)$ of the intermediate scattering function. One of the points we make is that, in the present formalism, the first cumulant can be expressed in terms of the static form factor $S(q)$, when the Kirkwood–Riseman diffusion equation is used to describe chain dynamics. This feature enables one to include the effect of stiffness in the calculation of $\Omega(q)$, through the equilibrium distribution function involved in $S(q)$. Both broken-chain and sliding-rod models have been used to include the stiffness in the equilibrium distribution function.

Here we present the conclusions obtained with the sliding-rod model in which we treat a section of the chain of length bn as a rod. It has been shown that the usual intermediate-q region, where $qb \to 0$ and $qR_G \to \infty$, is divided into two subasymptotic regions. The first covers the q values for which $qbn \ll 1$ but $qR_G \gg 1$. In this region, the polymer behaves as a flexible chain and the first cumulant Ω tends to $\Omega \sim q^3$. In the second region, where $qb \ll 1$ but $qbn \gg 1$, the chain behaves as a rod and Ω tends to $\Omega \sim q^3 \ln (1/qb)$. One observes that the simple power law behavior does not prevail in this region due to the logarithmic factor.

These conclusions are particularly important in the interpretation of neutron scattering experiments, in which qbn may be of the order or larger than unity. It seems that in these experiments, if the chain is sufficiently stiff, the data are likely to fall in the q region corresponding to rodlike behavior (i.e., the second asymptotic region) or to the transition from flexible to rodlike behavior.

In the light scattering experiments with large molecules, for which $qR_G \gg 1$, the results are more likely to fall in the q region corresponding to the flexible-chain behavior.

The curves representing the variation of the first cumulant with the stiffness characterized by n may give an indication of what to expect in the intermediate-q region when the chain stiffness is varied in an experiment. These curves are expected to be particularly useful in the case of polyelectrolytes, where the stiffness may be controlled by adjusting the ionic strength of the solution.

In the light of the present and our earlier work, we are led to conclude that the interpretation of the scattering data in the intermediate-q region requires the inclusion of chain stiffness and hydrodynamic strength as adjustable parameters.

Acknowledgment. M.D. acknowledges the support received from the Macromolecular Research Center during his stay at The University of Michigan in Jan 1980. Acknowledgment is made to the donors of the Petroleum Research Fund, administered by the American Chemical Society, for partial support.

Appendix I. Derivation of Equation 5

In this appendix we present the main steps used in the derivation of (5) from (4). First we write eq 4 in the form

$$\langle \rho^*\rho \rangle = 1 + 2\mathrm{DS} + \mathrm{FS} \qquad (\mathrm{I.1})$$

where

$$\mathrm{DS} = \sum_{j=1}^{N} \sum_{\alpha=0}^{n-1} \langle e^{i\mathbf{q}\cdot(\mathbf{R}_N - \mathbf{R}_j - \alpha\mathbf{b}_j)} \rangle$$

and

$$\mathrm{FS} = \sum_{j=1}^{N} \sum_{\alpha=0}^{n-1} \sum_{l=1}^{N} \sum_{\beta=0}^{n-1} \langle e^{i\mathbf{q}\cdot(\mathbf{R}_j - \mathbf{R}_l + \alpha\mathbf{b}_j - \beta\mathbf{b}_l)} \rangle$$

FS can be split into two parts accounting for $j = l$ and $j \neq l$

$$\mathrm{FS} = \sum_{j=1}^{N} \sum_{\alpha\beta=0}^{n-1} \langle e^{i\mathbf{q}\cdot\mathbf{b}_j(\alpha-\beta)} \rangle + 2 \sum_{j>l} \sum_{\alpha\beta=0}^{n-1} \langle e^{i\mathbf{q}\cdot(\sum_{m=l}^{j-1}\mathbf{B}_m + (\alpha/n)\mathbf{B}_j - (\beta/n)\mathbf{B}_l)} \rangle \qquad (\mathrm{I.2})$$

where we have used

$$\mathbf{R}_j - \mathbf{R}_l \equiv \sum_{m=l}^{j-1} \mathbf{B}_m$$

$$\mathbf{B}_m \equiv \mathbf{R}_{m+1} - \mathbf{R}_m \equiv n\mathbf{b}_m$$

The second term in (I.2) involves a fourth-order summation which can be written as

$$\sum_{j>l} \sum_{\alpha\beta} \langle --- \rangle = \sum_{l=1}^{N} \sum_{\alpha\beta=0}^{n-1} \langle e^{i\mathbf{q}\cdot[(\alpha/n)\mathbf{B}_{l+1} + (1-\beta/n)\mathbf{B}_l]} \rangle + \sum_{l=1}^{N} \sum_{j=l+2}^{N} \sum_{\alpha\beta=0}^{n-1} \langle e^{i\mathbf{q}\cdot[\sum_{m=l+1}^{j-1}\mathbf{B}_m + (\alpha/n)\mathbf{B}_j + (1-\beta/n)\mathbf{B}_l]} \rangle$$

Performing the averages with respect to the distribution of $\mathbf{B}_m$

$$P(\{\mathbf{B}\}^N) = \left(\frac{1}{4\pi n^2 b^2}\right)^N \prod_{m=1}^{N} \delta(|\mathbf{B}_m| - nb)$$

we obtain

$$\sum_{j>l} \sum_{\alpha\beta} \langle --- \rangle = \frac{1}{2} \sum_{jl=1}^{N}{}' \left(\frac{\sin (qbn)}{qbn}\right)^{|j-l|-1} \left(\sum_{\alpha=0}^{n-1} \frac{\sin (qb\alpha)}{qb\alpha}\right) \times \left(\sum_{\beta=1}^{n} \frac{\sin (qb\beta)}{qb\beta}\right) \qquad (\mathrm{I.3})$$

where we have used

$$\sum_{j=l+2}^{N} \left(\frac{\sin (qbn)}{qbn}\right)^{j-l-1} = \frac{1}{2} \sum_{j(\neq l)} \left(\frac{\sin (qbn)}{qbn}\right)^{|j-l|-1} - 1$$

Combining (I.2) and (I.3) we arrive at the result

$$\mathrm{FS} = N \sum_{\alpha\beta=0}^{n-1} \frac{\sin [qb(\alpha-\beta)]}{qb(\alpha-\beta)} + \sum_{jl=1}^{N}{}' \left(\frac{\sin (qbn)}{qbn}\right)^{|j-l|-1} \left(\sum_{\alpha=0}^{n-1} \frac{\sin (qb\alpha)}{qb\alpha}\right) \left(\sum_{\beta=1}^{n} \frac{\sin (qb\beta)}{qb\beta}\right) \qquad (\mathrm{I.4})$$

Consider now the double sum DS and use the same procedure as in FS

$$\mathrm{DS} = \sum_{j=1}^{N} \sum_{\alpha=0}^{n-1} \langle e^{i\mathbf{q}\cdot[\sum_{m=j+1}^{N}\mathbf{B}_m + (n-\alpha)\mathbf{b}_j]} \rangle$$

or

$$\mathrm{DS} = \sum_{j=1}^{N} \left(\frac{\sin (qbn)}{qbn}\right)^{j-1} \left(\sum_{\alpha=1}^{n} \frac{\sin (qb\alpha)}{qb\alpha}\right) \qquad (\mathrm{I.5})$$

Combining (I.1), (I.4), and (I.5) we obtain the static form factor as

$$\langle \rho^* \rho \rangle = 1 + NS_n^{\mathrm{rod}}(qb) + j_0^{-1}(qbn)S[S + 1 - j_0(qbn)] \sideset{}{'}\sum_{jl=1}^{N} j_0^{|j-l|}(qbn) + 2S\,\frac{1 - j_0^{N}(qbn)}{1 - j_0(qbn)} \quad \text{(I.6)}$$

The notation used in (I.6) is defined in eq 5. We can reduce double summations into single ones as

$$\sum_{\alpha\beta=0}^{n-1} j_0[qb(\alpha - \beta)] \equiv S_n^{\mathrm{rod}}(qb)$$

$$= n + 2\sum_{\alpha=1}^{n} (n - \alpha) j_0(qb\alpha)$$

and

$$\sideset{}{'}\sum_{jl=1}^{N} j_0^{|j-l|}(qbn) = 2\sum_{l=1}^{N-1} (N - l) j_0^{l}(qbn)$$

which we can cast in the following form by using simple algebraic transformations:

$$\sideset{}{'}\sum_{jl=1}^{N} j_0^{|j-l|}(qbn) = 2N\left\{G_N(j_0(qbn)) - \frac{j_0(qbn)[1 - j_0^{N}(qbn)]}{N[1 - j_0(qbn)]}\right\} \quad \text{(I.7)}$$

where $G_N(x)$ is defined in eq 5. Substituting (I.7) in (I.6) we arrive at eq 5.

Appendix II. Calculation of the Integral in Equation 21

In this appendix we want to calculate the integral

$$I(\epsilon) = \int_{\epsilon}^{\infty} \frac{\mathrm{d}x}{x^2}\left[\sin x - \frac{(\sin x - x\cos x)}{x^2}\right]$$

$$= \frac{1}{4}\int_{\epsilon}^{\infty} \frac{\mathrm{d}x}{x} \int_{-1}^{1} \mathrm{d}\mu\,(1 + \mu^2)e^{ix\mu} \quad \text{(II.1)}$$

where $\epsilon \equiv qb$ and tends to zero.

Performing the μ integration by parts, it is easy to verify that

$$\int_{-1}^{1} \mathrm{d}\mu\,(1 + \mu^2)e^{ix\mu} = \frac{8}{3}\cos x + 2x\int_{0}^{1} \mathrm{d}\mu\,\mu\left(1 + \frac{\mu^2}{3}\right)\sin(\mu x)$$

and substituting this into (II.1) we obtain

$$I(\epsilon) = \frac{2}{3}\int_{\epsilon}^{\infty} \mathrm{d}x\,\frac{\cos x}{x} + \frac{1}{2}\int_{0}^{1} \mathrm{d}\mu\left(1 + \frac{\mu^2}{3}\right) \quad \text{(II.2)}$$

where we have let $\epsilon \rightarrow 0$ and used

$$\int_{0}^{\infty} \mathrm{d}x\,\sin(\mu x) = \lim_{s\to 0} \frac{\mu}{\mu^2 + s^2} = \frac{1}{\mu}$$

We can reduce (II.2) as follows:

$$I(\epsilon) = \frac{5}{9} - \frac{2}{3}\,\mathrm{ci}\,(\epsilon) \quad \text{(II.3)}$$

where ci (ϵ) is the cosine integral[30]

$$\mathrm{ci}\,(\epsilon) = -\int_{\epsilon}^{\infty} \mathrm{d}x\,(\cos x/x)$$

$$= 0.577 + \ln \epsilon + \int_{0}^{\epsilon} \mathrm{d}x\,\frac{\cos x - 1}{x}$$

When $\epsilon \rightarrow 0$

$$I(\epsilon) \approx (2/3)\ln(1/\epsilon)$$

which yields eq 22.

Appendix III. Derivation of Equation 43

For a broken chain of $\mathcal{N}$ monomers, R_{G} is given by

$$2\mathcal{N}^2 R_{\mathrm{G}}^2 = \mathrm{FT} + 2\mathrm{ST} + 2\mathrm{TT} \quad \text{(III.1)}$$

where

$$\mathrm{FT} = N\sum_{\alpha\beta=0}^{n-1} \langle |\mathbf{R}_\alpha - \mathbf{R}_\beta|^2 \rangle$$

which can immediately be calculated as

$$\mathrm{FT} = Nb^2 \sum_{\alpha\beta=0}^{n-1} (\alpha - \beta)^2 \quad \text{(III.2)}$$

$$\mathrm{ST} = \sum_{j>l}\sum_{\alpha\beta}\left\langle \left|\sum_{m=l}^{j-1} \mathbf{B}_m + \frac{\alpha}{n}\mathbf{B}_j - \frac{\beta}{n}\mathbf{B}_l\right|^2 \right\rangle$$

and

$$\mathrm{TT} = \sum_{l\beta}\left\langle \left|\sum_{m=l}^{N} \mathbf{B}_m - \frac{\beta}{n}\mathbf{B}_l\right|^2 \right\rangle$$

with

$$\mathbf{R}_j - \mathbf{R}_l \equiv \sum_{m=l}^{j-1} \mathbf{B}_m$$

Expand ST summation into two parts as follows:

$$\mathrm{ST} = \sum_{l=1}^{N}\sum_{\alpha\beta}\left\langle \left|\frac{\alpha}{n}\mathbf{B}_{l+1} + \left(1 - \frac{\beta}{n}\right)\mathbf{B}_l\right|^2 \right\rangle + \sum_{l=1}^{N}\sum_{j=l+2}^{N}\sum_{\alpha\beta}\left\langle \left|\sum_{m=l+1}^{j-1} \mathbf{B}_m + \frac{\alpha}{n}\mathbf{B}_j + \left(1 - \frac{\beta}{n}\right)\mathbf{B}_l\right|^2 \right\rangle$$

Using similar arguments to those in Appendix I, we can verify

$$\mathrm{ST} = \frac{n^2 b^2}{2} \sideset{}{'}\sum_{jl=1}^{N} \sum_{\alpha\beta=0}^{n-1} \left[|j - l| - 1 + \frac{\alpha^2}{n^2} + \left(1 - \frac{\beta}{n}\right)^2 \right] \quad \text{(III.3)}$$

TT can be calculated in much the same way as ST and the result is

$$\mathrm{TT} = n^2 b^2 \sum_{l=1}^{N} \sum_{\beta=0}^{n-1} \left[l - 1 + \left(1 - \frac{\beta}{n}\right)^2 \right] \quad \text{(III.4)}$$

Combining (III.1) to (III.4) we obtain

$$R_{\mathrm{G}}^2 = \frac{Nb^2}{2\mathcal{N}^2}\sum_{\alpha\beta=0}^{n-1} (\alpha - \beta)^2 + \frac{b_2}{2\mathcal{N}^2} \sideset{}{'}\sum_{jl=1}^{N} \sum_{\alpha\beta=0}^{n-1} [n^2|j - l| + (\alpha - \beta)^2 - 2\beta(n - \alpha)] + \frac{b^2}{\mathcal{N}^2}\sum_{l=1}^{N}\sum_{\alpha\beta=0}^{n-1} [n^2(l - 1) + (n - \beta)^2] \quad \text{(III.5)}$$

Using the transformations[30]

$$\sum_{\alpha\beta=0}^{n-1} (\alpha - \beta)^2 = 2\sum_{\alpha=1}^{n-1} (n - \alpha)\alpha^2$$

$$\sum_{jl=1}^{N} |j - l| = 2\sum_{j=1}^{N-1} (N - j)j$$

$$\sum_{\alpha=1}^{n-1} \alpha^2 = n(n - 1)(2n - 1)/6$$

$$\sum_{\alpha=1}^{n-1} \alpha^3 = [n(n-1)/2]^2$$

and combining certain terms together we arrive at (43) in the text.

References and Notes

(1) Daoud, M. Thesis, Université de Paris IV, 1977.

(2) de Gennes, P. G. "Scaling Concepts in Polymer Physics"; Cornell University Press: Ithaca, N.Y., 1979.

(3) Yamakawa, H. "Modern Theory of Polymer Solutions"; Harper and Row: New York, 1971.

(4) Kitano, T.; Taguchi, A.; Noda, I.; Nagasawa, M. *Macromolecules* **1980**, *13*, 57.

(5) Kratky, O.; Porod, G. *Recl. Trav. Chim. Pays-Bas* **1949**, *68*, 1106.

(6) Hermans, J. J.; Ullman, R. *Physica* **1952**, *18*, 951.

(7) Koyama, R. *J. Phys. Soc. Jpn.* **1973**, *34*, 1029.

(8) Norisuye, T.; Murakama, H.; Fujita, H. *Macromolecules* **1978**, *11*, 966.

(9) Akcasu, Z.; Benmouna, M.; Han, C. C. *Polymer* **1980**, *21*, 866. *Polymer.*

(10) Richter, D.; Hayter, J.; Mezei, R.; Ewen, B. *Phys. Rev. Lett.* **1978**, *41*, 1484.

(11) Akcasu, Z.; Gurol, H. *J. Polym. Sci., Polym. Phys. Ed.* **1976**, *14*, 1.

(12) Benmouna, M.; Akcasu, Z. *Macromolecules* **1978**, *11*, 1187.

(13) Akcasu, Z.; Benmouna, M. *Macromolecules* **1978**, *11*, 1193.

(14) Benmouna, M.; Akcasu, Z. *Macromolecules* **1980**, *13*, 409.

(15) (a) Schmidt, M.; Burchard, W. *Macromolecules* **1978**, *11*, 460. (b) Stockmayer, W. H.; Schmidt, M.; Burchard, W. *Ibid.* **1980**, *13*, 580. (c) Burchard, W.; Schmidt, M.; Stockmayer, W. H. *Ibid.* **1980**, *13*, 1265.

(16) Riseman, J.; Kirkwood, J. G. "Rheology, Theory and Applications"; Academic Press: New York, 1956.

(17) Hearst, J. E.; Stockmayer, W. H. *J. Chem. Phys.* **1962**, *37*, 1425.

(18) Stockmayer, W. H.; Burchard, W. *J. Chem. Phys.* **1979**, *70*, 3138.

(19) Fixman, M.; Kovac, J. *J. Chem. Phys.* **1974**, *61*, 4939.

(20) Helfand, E. *J. Chem. Phys.* **1979**, *71*, 5000.

(21) Akcasu, Z.; Higgins, J. S. *J. Polym. Sci., Polym. Phys. Ed.* **1977**, *15*, 1745.

(22) Berne, B. J.; Pecora, R. "Dynamic Light Scattering"; Wiley: New York, 1976.

(23) Fixman, M.; Skolnick, J. *Macromolecules* **1978**, *11*, 863.

(24) Akcasu, Z., to be submitted for publication.

(25) Burgers, J. M. "Second Report on Viscosity and Plasticity"; 1938; Vol. 16, p 1.

(26) Wilson, R.; Bloomfield, V. *Biopolymers* **1979**, *18*, 1205.

(27) Broersma, S. *J. Chem. Phys.* **1959**, *32*, 1626.

(28) Akcasu, Z.; Han, C. C. *Macromolecules* **1979**, *12*, 276.

(29) Benoit, H.; Doty, P. *J. Phys. Chem.* **1953**, *57*, 958.

(30) Gradhteyn, I. S.; Ruzlik, I. M. Eds. "Tables of Integrals, Series, and Products"; Academic Press: New York, 1965.

(31) Zimm, B. H.; Stein, R. S.; Doty, P. *Polym. Bull.* **1945**, *1*, 90.

(32) Fixman, M., to be submitted for publication (private communication).

Notes

Second Moment of Finite Polymer Chains

KEIZO MATSUO

Department of Chemistry, Dartmouth College, Hanover, New Hampshire 03755. *Received April 29, 1980*

A relatively simple formulation of the second moment of *infinite* polymer chains with repeat units of any size has been given.[1] In order to calculate unperturbed chain dimensions or dipole moments of *finite* linear chains, the so-called generalized method[2] by Flory and Jernigan must be used. However, the generalized method requires 15 × 15 matrices in the case of a three-state rotational isomeric state (RIS) model, while for the older methods proposed by Lifson,[3] Nagai,[4] and Hoeve,[5] 9 × 9 matrices are sufficient to get second moments of *infinite* polymer chains. We present here a formula with 9 × 9 matrices which gives very close approximations to the second moments of *finite* polymer chains.

Again it seems unnecessary to give a detailed derivation since this exercise can be performed by straightforward generalization of previously published results for two-[6] and three-bond[7] repeat units, taking account of the general properties[8] of the RIS model. The notation used here is precisely that of Flory's book[8] unless otherwise stated. Let there be s bonds within a repeat unit, numbered by indices α or β running from 1 to s. With x denoting the number of repeat units of a chain, the formula of the second moment then reads

$$\langle M^2\rangle/x = \sum_{\alpha=1}^{s} m_\alpha{}^2 + (2/x) \sum_{\alpha,\beta=1}^{s} \mathbf{m}_\alpha{}^{\mathrm{T}}(\mathbf{B}_\alpha{}^* \otimes \mathbf{E}_3) \times [(x-1)\mathbf{E}_{3\nu} - x\mathbf{S}_\alpha + \mathbf{S}_\alpha{}^x](\mathbf{E}_{3\nu} - \mathbf{S}_\alpha)^{-2}\mathbf{R}_{\alpha\beta}(\mathbf{A}_\alpha \otimes \mathbf{E}_3)\mathbf{m}_\beta \quad (1)$$

When $\alpha < \beta$, x should be replaced by $x + 1$. Definitions of several symbols appearing in the formula can be found in detail in the previous paper.[1]

This formula is not an *exact* expression of the second moments of *finite* chains (because the largest eigenvalue has been used for normalization instead of the complete partition function). The generalized method, on the other hand, yields an exact expression, however.[8] When x ($=n$ for $s = 1$) is smaller than 10, there still remains a difference between the generalized and the eigenvalue method due to some end-group contributions and to the difference between the partition function and the largest eigenvalues. However, these become relatively small as x increases. This method is expected to give excellent results in all cases where the largest eigenvalue of $\mathbf{Q}\alpha$ (U matrices) is much larger than the other ones. If, however, this is not the case, convergence to the correct result is a bit slower. Readers are well-advised to refer to Nagai's earlier work[9] on the second and higher even moments using the largest eigenvalue method.

A small rearrangement of eq 1 gives

$$\langle M^2\rangle/x = \lim_{x\to\infty} \langle M^2\rangle/x - (2/x) \sum_{\alpha,\beta=1}^{s} \mathbf{m}_\alpha{}^{\mathrm{T}}(\mathbf{B}_\alpha{}^* \otimes \mathbf{E}_3) \times (\mathbf{E}_{3\nu} - \mathbf{S}_\alpha{}^x)(\mathbf{E}_{3\nu} - \mathbf{S}_\alpha)^{-2}\mathbf{R}_{\alpha\beta}(\mathbf{A}_\alpha \otimes \mathbf{E}_3)\mathbf{m}_\beta \quad (2)$$

where $\lim_{x\to\infty} \langle M^2\rangle/x$ can be obtained directly from our earlier result.[1]

Flory and Jernigan's method[2] requires 21 × 21 matrices for a three-state RIS model to evaluate the mean-square radius of gyration. Here again a slightly simpler formula is proposed, with only 9 × 9 matrices, to calculate a mean-square radius of gyration. Though the formula does not give an exact expression because of the reasons stated earlier, it reproduces more than 99% of an exact value obtained by Flory and Jernigan's method. The derivation *of this formula is relatively straightforward (from the series* of expansions of $\langle s^2\rangle_0 = (n+1)^{-2}\sum_{0\le h\le k\le n}\sum_{i=h+1}^{k}\cdot\sum_{j=h+1}^{k}\langle \mathbf{l}_i\cdot\mathbf{l}_j\rangle$, numerical orders were obtained). Again the

0024-9297/80/2213-1712$01.00/0